

# A Global-in-time Domain Decomposition Method for the Coupled Nonlinear Stokes and Darcy Flows

Thi-Thao-Phuong Hoang<sup>1</sup> • Hyesuk Lee<sup>2</sup>

Received: 22 April 2020 / Revised: 10 October 2020 / Accepted: 6 February 2021 / Published online: 2 March 2021 © The Author(s), under exclusive licence to Springer Science+Business Media, LLC part of Springer Nature 2021

#### **Abstract**

We study a decoupling iterative algorithm based on domain decomposition for the time-dependent nonlinear Stokes–Darcy model, in which different time steps can be used in the flow region and in the porous medium. The coupled system is formulated as a space-time interface problem based on the interface condition for mass conservation. The nonlinear interface problem is then solved by a nested iteration approach which involves, at each Newton iteration, the solution of a linearized interface problem and, at each Krylov iteration, parallel solution of time-dependent linearized Stokes and Darcy problems. Consequently, local discretizations in time (and in space) can be used to efficiently handle multiphysics systems of coupled equations evolving at different temporal scales. Numerical results with nonconforming time grids are presented to illustrate the performance of the proposed method.

**Keywords** Stokes—Darcy coupling  $\cdot$  Non-Newtonian fluids  $\cdot$  Domain decomposition  $\cdot$  Local time-stepping  $\cdot$  Space-time interface problem  $\cdot$  Nested iteration

Mathematics Subject Classification 65N30 · 76D07 · 76S05 · 65M55

#### 1 Introduction

Multiscale and multiphysics processes are ubiquitous in many science and engineering applications. Mathematically, coupled partial differential equations are used to model various processes possibly taking place on different regions of the problem domain and at different

hklee@clemson.edu

School of Mathematical and Statistical Sciences, Clemson University, Clemson, SC 29634, USA



T.-T.-P. Hoang's work is partially supported by the US National Science Foundation under grant number DMS-1912626 and Auburn University's intramural grants program.

H. Lee's work is partially supported by the US National Science Foundation under grant number DMS-1818842.

<sup>☑</sup> Thi-Thao-Phuong Hoang tzh0059@auburn.eduHyesuk Lee

Department of Mathematics and Statistics, Auburn University, Auburn, AL 36849, USA

scales in space and time. One example of such a coupling is the coupled (Navier-)Stokes—Darcy system arising in a number of applications: surface and subsurface flow interaction, flow in vuggy porous media, industrial filtrations, biofluid-organ interaction, cardiovascular flows, and others. In these applications, the Stokes equations are used to model the free flow and the Darcy equations are used to model the flow in a porous medium; the two flow domains are coupled via suitable transmission conditions on the interface to enforce mass conservation, balance of the normal forces and the Beavers–Joseph–Saffman law [4,47,61].

The development of numerical approximations and efficient solvers for the Stokes–Darcy coupling has been an active research area and attracted great attention over the past two decades. For the stationary case, the existence and uniqueness of the weak solution of the coupled system are proved in [5,24,27,49]. Regarding a numerical solution of the mixed Stokes-Darcy model, one can either solve the coupled system directly with some suitable preconditioner, or use the domain decomposition (DD)-based approach [56,64] to decouple the system into two local subsystems which are solved separately. Concerning the former or monolithic approach, new finite element spaces were studied in [1,2,7,52] with mixed formulations and in [57,58] with discontinuous approximations. Preconditioning techniques for solving the sparse linear system of saddle point form resulted from finite element discretization of the fully coupled Stokes-Darcy system were investigated in [10,19,53]. Concerning the decoupled approach, several directions have been considered. Lagrange multiplier techniques were proposed in [30,49] and mortar finite elements were studied in [5,31,36,37,39] in which the meshes on the interface and subregions do not necessarily match. Heterogeneous DD methods were explored using either the classical Dirichlet–Neumann (Steklov–Poincaré) type operator [24–26,38,46,66] or the Robin–Robin interface conditions [11,12,18,23,28]. Two-grid methods were applied to the mixed Stokes–Darcy model in [8,54], and optimizationbased approach was proposed in [29].

While quite extensive work has been devoted to the analysis and numerical solution methods to the steady Stokes-Darcy system, only a few studies have been carried out for the nonsteady case. Basically, there are two approaches that were proposed for the timedependent Stokes-Darcy coupling: the first one is based on implicit time discretization as presented in [15,24], in which at each time step the system is solved directly or is uncoupled by DD iteration. The second approach is a decoupled method obtained by lagging the interface coupling terms, i.e. at each time level, one solves the Stokes and Darcy problems implicitly using Neuman interface boundary conditions computed from the previous time level. Such a method was first introduced in [55] using the backward Euler method in time. The conditional stability of the method and a modified two-step method was analyzed in [50]. A similar decoupled scheme with Robin interface conditions was studied in [13] in which higher order time discretization (three-step backward differentiation method) was also considered. It should be noted that in these works, the same time step is used in both regions. Decoupled schemes with different time step sizes were proposed and analyzed in [60,62]. These schemes are extensions of the method in [55] in which the time step size in the Stokes region is an integral multiple of the time step size in the Darcy region. The advancement in time is then carried out sequentially; first the Stokes problem is solved with a small time step size using the Darcy pressure (freezing from the previous coarse time step) as interface data, then the Darcy problem is solved using the recently computed Stokes velocity as interface data. These methods are non-iterative by using an explicit method for the coupling terms, and the key issue is how to achieve desired accuracy and stability properties. A different approach was proposed in [51] by formulating the coupled problem as a constrained optimal control problem which is solved at each time step by a least square method (thus, the same time step is used in both regions).



As the model concerns the flow of fluid, there are two possible fluid types: Newtonian fluids (e.g. water and air) and non-Newtonian fluids (e.g. honey and quicksand). The difference between these two types of fluid lies in the viscosity which is a constant for Newtonian fluids and a function of the magnitude of the deformation tensor for non-Newtonian fluids (more discussion can be found in [30]). Mathematically, one deals with a linear or nonlinear coupled flow problem; the nonlinear Stokes–Darcy coupling was considered in [29–31,51]. In addition, approximation methods for the nonlinear Navier-Stokes/Darcy system were studied in [3,9,17,20,21,28,40], and for the coupling with transport in [16,59,65].

In this work, we aim to develop a parallel decoupling method for the time-dependent nonlinear Stokes-Darcy system in which different time step sizes can be used in the free flow domain and the porous medium. Differently from [60,62], we apply the so-called global-in-time (or space-time) DD method in which the dynamic system is decoupled into dynamic subsystems defined on the subdomains (resulting from a spatial decomposition), then time-dependent problems are solved in each subdomain at each iteration and information is exchanged over space-time interfaces between subdomains. Consequently, local discretizations in both space and time can be enforced in different regions of the computational domain, which makes the method well-suited and efficient for multiscale multiphysics problems. Though the space-time DD methods have been extensively studied for porous medium flows (see [43,44] and the references therein), the application of these methods to multiphysics problems is still limited; to the best of our knowledge, these methods haven't been considered for the Stokes-Darcy coupling in the literature. It is noteworthy that, unlike the explicit-implicit method in [60,62], space-time DD is fully implicit in time, thus not only different time steps can be used, but also considerably large time step sizes are possible without affecting stability. This feature is strongly desired for applications in geosciences where long time simulations are often required. In addition, an important class of global-in-time DD methods is the so-called Optimized Schwarz Waveform Relaxation (OSWR) method [32–34,41] in which, instead of using the physical transmission conditions, general (Robin or Ventcell [108]) transmission operators are employed to enhance the information exchange between subdomains. These new transmission conditions involve some coefficients that can be optimized to improve the convergence rates of the iterations.

This work aims to develop and investigate the space-time DD method for the nonlinear Stokes-Darcy system based on the physical transmission conditions. Specifically, we construct a time-dependent Steklov-Poincaré type operator, and reduce the coupled problem into a nonlinear time-dependent interface problem enforcing the continuity of the normal velocity along the interface. Such an interface problem is then solved by a nested iteration approach which involves, at each Newton iteration, the solution of a linearized interface problem and, at each Krylov iteration, parallel solution of time-dependent linearized Stokes and Darcy problems. As the local problems are solved globally and implicitly in time at each iteration, it makes possible the use of different time discretization methods or different time grids in the Stokes and Darcy regions, and the time step sizes can be large for long-term simulations. To exchange information at the interface with nonconforming time grids, an  $L^2$  time projection between subdomains is performed by an optimal projection algorithm without any additional grid [35]. High order time stepping methods can be applied straightforwardly, see [41]. The idea can be generalized to the case of multiple subdomains where interfaces of different types are introduced: Stokes-Darcy, Stokes-Stokes and Darcy-Darcy as considered in [66] for the steady problems. However, in this work we restrict ourselves to the case of two subdomains and conforming spatial meshes, and focus on numerical performance - in terms of accuracy and efficiency - of the proposed method with nonmatching time grids. The study of the Schwarz waveform relaxation method for the



Stokes–Darcy coupling with Robin transmission conditions will be considered separately in [45].

The rest of this paper is structured as follows. In Sect. 2, we present the model problem which is the nonstationary nonlinear Stokes–Darcy system, and the interface coupling conditions. The variational formulation of the continuous coupled system is derived in Sect. 3. The coupled problem is formulated as a time-dependent nonlinear interface problem in Sect. 4, and nonconforming time discretization is discussed in Sect. 5. Numerical results are presented in Sect. 6 to study the performance of the proposed algorithm with nonmatching time grids, and with large jumps in the coefficients and long time horizons. Finally, some concluding remarks are given in Sect. 7.

## 2 Time-Dependent Nonlinear Stokes-Darcy System

We consider a free non-Newtonian fluid flow in  $\Omega_f$  coupled with a porous medium flow in  $\Omega_p$ , where  $\Omega_f$  and  $\Omega_p$  are subsets of  $\mathbb{R}^d$  for d=2,3. Denote by  $\Gamma$  the interface between the two domains, and by  $\Gamma_f=\partial\Omega_f\backslash\Gamma$  and  $\Gamma_p=\partial\Omega_p\backslash\Gamma$  the external boundaries of the fluid domain and porous medium, respectively (see Fig. 1). Let  $\mathbf{n}_f$  and  $\mathbf{n}_p$  be the outward unit normal vectors to  $\Omega_f$  and  $\Omega_p$  respectively, and  $\{\mathbf{t}_j\}_{j=1,\dots,d-1}$  be an orthogonal set of unit tangent vectors on  $\Gamma$ . Let T>0 be a finite time. The free flow in  $\Omega_f$  is described by the nonlinear Stokes equations subject to no-slip boundary condition on  $\Gamma_f$ :

$$\frac{\partial \boldsymbol{u}_f}{\partial t} - \nabla \cdot \boldsymbol{T}(\boldsymbol{u}_f, p_f) = \boldsymbol{f}_f \quad \text{in } \Omega_f \times (0, T), \tag{2.1a}$$

$$\nabla \cdot \boldsymbol{u}_f = 0 \quad \text{in } \Omega_f \times (0, T), \tag{2.1b}$$

$$\mathbf{u}_f = \mathbf{0} \quad \text{on } \Gamma_f \times (0, T), \tag{2.1c}$$

$$\mathbf{u}_f(\cdot,0) = \mathbf{u}_{f0} \quad \text{in } \Omega_f, \tag{2.1d}$$

where  $\mathbf{u}_f$  is the fluid velocity,  $p_f$  the fluid pressure,  $\mathbf{T}(\mathbf{u}_f, p_f) = v_f(|\mathbf{D}(\mathbf{u}_f)|)\mathbf{D}(\mathbf{u}_f) - p_f\mathbf{I}$  the stress tensor (with  $\mathbf{I}$  the identity tensor),  $\mathbf{D}(\mathbf{u}_f) = \frac{1}{2} \left( \nabla \mathbf{u}_f + \nabla \mathbf{u}_f^T \right)$  the rate of the strain tensor,  $v_f(\cdot)$  the fluid viscosity and  $\mathbf{f}_f$  the body force. In this work we consider the Cross model for the viscosity function:

$$\nu_f(|\boldsymbol{D}(\boldsymbol{u}_f)|) = \nu_{f\infty} + \frac{\nu_{f0} - \nu_{f\infty}}{1 + K_f |\boldsymbol{D}(\boldsymbol{u}_f)|^{2-r_f}},$$
(2.2)

where  $r_f > 1$ ,  $v_{f\infty}$ ,  $v_{f0} > 0$  and  $K_f > 0$  are constants;  $v_{f\infty}$  and  $v_{f0}$  denote the limiting viscosity values at an infinite shear rate and at zero shear rate respectively, and satisfy  $v_{f\infty} \le v_{f0}$ . Other nonlinear viscosity models such as Carreau model, power law model and Ladyzhenskaya model can also be used [30].

The porous medium flow in  $\Omega_p$  is described by the nonlinear Darcy equations subject to no-flux boundary condition on  $\Gamma_p$ :

$$\nu_{\text{eff}}(|\boldsymbol{u}_p|) \kappa^{-1} \boldsymbol{u}_p + \nabla p_p = 0 \quad \text{in } \Omega_p \times (0, T), \tag{2.3a}$$

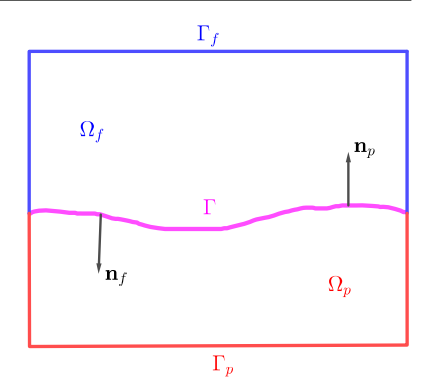
$$S_p \frac{\partial p_p}{\partial t} + \nabla \cdot \boldsymbol{u}_p = f_p \quad \text{in } \Omega_p \times (0, T), \tag{2.3b}$$

$$\boldsymbol{u}_p \cdot \boldsymbol{n}_p = 0 \quad \text{on } \Gamma_p \times (0, T),$$
 (2.3c)

$$p_p(\cdot, 0) = p_{p0} \quad \text{in } \Omega_p, \tag{2.3d}$$



Fig. 1 Example of a two dimensional domain formed by a fluid region and a porous medium



where  $\mathbf{u}_p$  and  $p_p$  are the Darcy velocity and pressure respectively,  $S_p > 0$  the storage coefficient,  $v_{\text{eff}}(\cdot)$  the effective fluid viscosity,  $\kappa > 0$  the permeability and  $f_p$  is the source/sink. The Cross model for  $v_{\text{eff}}$  is defined as follows (see [30] for other models):

$$\nu_{\text{eff}}(|\boldsymbol{u}_{p}|) = \nu_{p\infty} + \frac{\nu_{p0} - \nu_{p\infty}}{1 + K_{p}|\boldsymbol{u}_{p}|^{2 - r_{p}}},$$
(2.4)

where  $r_p > 1$ ,  $\nu_{p0} \ge \nu_{p\infty} > 0$  and  $K_p > 0$  are constants.

The viscosity functions (2.2) and (2.4) have the following properties which will be used in later analysis [30]:

- (A1)  $v_f(\cdot)$  and  $v_{\text{eff}}(\cdot)$  are strongly monotone and bounded from below and above by positive
- (A2) The nonlinear functions  $v_f(|\mathbf{u}|)|\mathbf{u}|$  and  $v_{\text{eff}}(|\mathbf{u}|)\mathbf{u}$  are uniformly continuous with respect to  $\boldsymbol{u} \in \mathbb{R}^d$ .

Note that the standard linear Stokes–Darcy system can be recovered by setting  $r_f = r_p = 2$ . The coupled Stokes-Darcy system is closed by the following coupling conditions on the space-time interface:

$$\mathbf{u}_f \cdot \mathbf{n}_f + \mathbf{u}_p \cdot \mathbf{n}_p = 0 \quad \text{on } \Gamma \times (0, T),$$
 (2.5a)

$$-\boldsymbol{n}_f \cdot (v_f(|\boldsymbol{D}(\boldsymbol{u}_f)|)\boldsymbol{D}(\boldsymbol{u}_f) - p_f \boldsymbol{I}) \cdot \boldsymbol{n}_f = p_p \text{ on } \Gamma \times (0, T),$$
(2.5b)

$$-\boldsymbol{n}_f \cdot (v_f(|\boldsymbol{D}(\boldsymbol{u}_f)|)\boldsymbol{D}(\boldsymbol{u}_f) - p_f \boldsymbol{I}) \cdot \boldsymbol{t}_j = c_{BJS}\boldsymbol{u}_f \cdot \boldsymbol{t}_j \quad \text{on } \Gamma \times (0,T), \ j = 1,\dots,d-1,$$
(2.5c)

where  $c_{BJS}$  is a positive constant. These coupling conditions have been studied extensively in the literature (e.g. [14,24,49]). The first two conditions enforce the continuity of the normal component of velocities and the continuity of the normal stress respectively. The third condition is the Beavers–Joseph–Saffmann condition [47,61], stating the connection between the slip velocity and the shear stress along the interface. It is a simplification of the Beavers-Joseph condition [4] by neglecting the porous medium velocity tangent to the interface. Thus (2.5c) is actually not a coupling condition as it only involves the fluid domain's variables. Next, we derive the weak formulation of the coupled system with the use of Lagrange multipliers.

## 3 Variational Formulation of the Fully Coupled System

In the following, we will use the convention that if V is a space of functions, then we write Vfor a space of vector functions having each component in V. In order to write the variational



formulation of the coupled problems, we first introduce the functional spaces:

$$\begin{aligned} & \boldsymbol{u}_f \in \boldsymbol{X}_f := \{ \boldsymbol{v} \in \boldsymbol{H^1}(\Omega_f) : \boldsymbol{v} = \boldsymbol{0} \text{ on } \Gamma_f \}, \quad p_f \in Q_f := L^2(\Omega_f), \\ & \boldsymbol{u}_p \in \boldsymbol{X}_p := \{ \boldsymbol{v} \in \boldsymbol{L^2}(\Omega_p) : \nabla \cdot \boldsymbol{v} \in L^2(\Omega_p), \ \boldsymbol{v} \cdot \boldsymbol{n}_p = 0 \text{ on } \Gamma_p \}, \quad p_p \in Q_p := L^2(\Omega_p). \end{aligned}$$

Let  $\Omega = \Omega_1 \cup \Omega_2 \cup \Gamma$  and define the spaces  $\boldsymbol{X}$  and Q on  $\Omega$  by  $\boldsymbol{X} = \boldsymbol{X}_f \times \boldsymbol{X}_p$  and  $Q = Q_f \times Q_p$  respectively. Denote by  $\boldsymbol{X}_f^*$  the dual space of  $\boldsymbol{X}_f$ . For a domain  $\Theta = \Omega_f$  or  $\Theta = \Omega_p$ , we denote by  $(\cdot, \cdot)_{\Theta}$  the  $L^2$  inner product over  $\Theta$ . As in the stationary case [30,49], we introduce the Lagrange multiplier  $\lambda$  on the interface representing:

$$\lambda = -\boldsymbol{n}_f \cdot (v_f(|\boldsymbol{D}(\boldsymbol{u}_f)|)\boldsymbol{D}(\boldsymbol{u}_f) - p_f \boldsymbol{I}) \cdot \boldsymbol{n}_f = p_p \text{ on } \Gamma \times (0, T).$$
 (3.1)

The space for the Lagrange multiplier is  $\Lambda := H_{00}^{1/2}(\Gamma)$  (see [49]). We denote by  $\Lambda^* := \left(H_{00}^{1/2}(\Gamma)\right)^*$  the dual space of  $\Lambda$  and by  $\langle \cdot, \cdot \rangle_{\Gamma}$  the duality pairing between  $\Lambda^*$  and  $\Lambda$ . Define the bilinear forms  $a(\cdot, \cdot) : \mathbf{X} \times \mathbf{X} \to \mathbb{R}$ ,  $b(\cdot, \cdot) : \mathbf{X} \times Q \to \mathbb{R}$  and  $b_I : \mathbf{X} \times \Lambda \to \mathbb{R}$  by:

$$a(\mathbf{u}, \mathbf{v}) = a_f(\mathbf{u}_f, \mathbf{v}_f) + a_p(\mathbf{u}_p, \mathbf{v}_p), \quad b(\mathbf{v}, q) = b_f(\mathbf{v}_f, q_f) + b_p(\mathbf{v}_p, q_p),$$

$$b_{\Gamma}(\mathbf{v}, \zeta) = b_{\Gamma f}(\mathbf{v}_f, \zeta) + b_{\Gamma p}(\mathbf{v}_p, \zeta),$$

where

$$a_{f}(\boldsymbol{u}_{f}, \boldsymbol{v}_{f}) = (v_{f}(|\boldsymbol{D}(\boldsymbol{u}_{f})|)\boldsymbol{D}(\boldsymbol{u}_{f}), \boldsymbol{D}(\boldsymbol{v}_{f}))_{\Omega_{f}} + \sum_{j=1}^{d-1} c_{BJS}(\boldsymbol{u}_{f} \cdot \boldsymbol{t}_{j}, \boldsymbol{v}_{f} \cdot \boldsymbol{t}_{j})_{\Gamma},$$

$$a_{p}(\boldsymbol{u}_{p}, \boldsymbol{v}_{p}) = (v_{\text{eff}}(|\boldsymbol{u}_{p}|) \kappa^{-1} \boldsymbol{u}_{p}, \boldsymbol{v}_{p})_{\Omega_{p}},$$

$$b_{f}(\boldsymbol{v}_{f}, q_{f}) = (q_{f}, \nabla \cdot \boldsymbol{v}_{f})_{\Omega_{f}}, \quad b_{p}(\boldsymbol{v}_{p}, q_{p}) = (q_{p}, \nabla \cdot \boldsymbol{v}_{p})_{\Omega_{p}},$$

$$b_{\Gamma f}(\boldsymbol{v}_{f}, \zeta) = \langle \zeta, \boldsymbol{v}_{f} \cdot \boldsymbol{n}_{f} \rangle_{\Gamma}, \quad b_{\Gamma p}(\boldsymbol{v}_{p}, \zeta) = \langle \boldsymbol{v}_{p} \cdot \boldsymbol{n}_{p}, \zeta \rangle_{\Gamma}.$$

The weak formulation of the coupled system (2.1)–(2.3)–(2.5) is then written as follows (detailed derivation for the stationary problems can be found in [30]): For a.e.  $t \in (0, T)$ , find  $(\mathbf{u}(t), p(t), \lambda(t)) \in \mathbf{X} \times Q \times \Lambda$  such that:

$$(\partial_{t}\boldsymbol{u}_{f},\boldsymbol{v}_{f})_{\Omega_{f}} + a(\boldsymbol{u},\boldsymbol{v}) - b(\boldsymbol{v},p) + b_{\Gamma}(\boldsymbol{v},\lambda) = (\boldsymbol{f}_{f},\boldsymbol{v}_{f})_{\Omega_{f}}, \qquad \forall \boldsymbol{v} \in \boldsymbol{X}, \quad (3.2)$$

$$b(\boldsymbol{u},q) - b_{\Gamma}(\boldsymbol{u},\zeta) + (S_{p}\partial_{t}p_{p},q_{p})_{\Omega_{p}} = (f_{p},q_{p})_{\Omega_{p}}, \quad \forall (q,\zeta) \in Q \times \Lambda, \quad (3.3)$$

with the initial conditions

$$\mathbf{u}_f(\cdot,0) = \mathbf{u}_{f0}$$
 in  $\Omega_f$ ,  $p_p(\cdot,0) = p_{p0}$  in  $\Omega_p$ .

The existence and uniqueness of the weak solution to the non-stationary and linear Stokes—Darcy system is proved in [14] using the Stokes—Laplace formulation, i.e. the velocity and pressure are the unknowns in the fluid flow domain and the pressure is the only unknown in the porous media domain. In addition, no Lagrange multiplier is introduced and the physically more accurate coupling condition - the Beavers—Joseph condition - is considered in [14]. The well-posedness of the stationary nonlinear Stokes—Darcy system in mixed form with a Lagrange multiplier is proved in [30]. Here we assume the variational formulation (3.2)—(3.3) is well-posed, and focus on the decoupled approach based on global-in-time domain decomposition.



## 4 Decoupled Problems and Nested Iteration Approach

We shall reformulate the Stokes-Darcy coupled problem as a space-time interface problem with the interface unknown  $\lambda$  defined in (3.1). Assume that  $\lambda$  is given, the Stokes and Darcy problems are then decoupled. We derive the weak formulations of the local problems using (3.1) as boundary conditions on the interface, then formulate the interface problem which is solved by a nested iteration approach.

#### 4.1 Free Fluid Flow

We first consider the Stokes problem with Neumann boundary condition on the interface  $\Gamma$ :

$$-\boldsymbol{n}_f \cdot (v_f(|\boldsymbol{D}(\boldsymbol{u}_f)|)\boldsymbol{D}(\boldsymbol{u}_f)) \cdot \boldsymbol{n}_f + p_f = \lambda, \quad \text{on } \Gamma \times (0, T).$$
(4.1)

Its variational formulation is given by:

For a.e.  $t \in (0, T)$ , find  $(\mathbf{u}_f(t), p_f(t)) \in \mathbf{X}_f \times Q_f$  such that:

$$(\partial_t \boldsymbol{u}_f, \boldsymbol{v}_f) + a_f(\boldsymbol{u}_f, \boldsymbol{v}_f) - b_f(\boldsymbol{v}_f, p_f) = (\boldsymbol{f}_f, \boldsymbol{v}_f)_{\Omega_f} - b_{\Gamma f}(\boldsymbol{v}_f, \lambda), \quad \forall \boldsymbol{v}_f \in \boldsymbol{X}_f,$$

$$(4.2)$$

$$b_f(\mathbf{u}_f, q_f) = 0, \qquad \forall q_f \in Q_f, \tag{4.3}$$

with the initial condition

$$\mathbf{u}_f(\cdot,0) = \mathbf{u}_{f0}, \quad \text{in } \Omega_f. \tag{4.4}$$

For given  $f_f \in L^2(0,T; \mathbf{X}_f^*)$ ,  $\lambda \in L^2(0,T;\Lambda)$  and  $\mathbf{u}_{f0} \in \mathbf{X}_f$ , the existence and uniqueness of the solution

$$(\boldsymbol{u}_f, p_f) \in (H^1(0, T; \boldsymbol{L^2}(\Omega_f) \cap L^2(0, T; \boldsymbol{X}_f)) \times L^2(0, T; Q_f)$$

to (4.2)–(4.3) with the initial condition (4.4) are followed from the strong monotonicity of the viscosity function (2.2), [31] and the classical result of wellposedness of evolutionary (Navier-)Stokes equations [63, Chapter III].

#### 4.2 Porous Medium Flow

We now consider the Darcy flow with Dirichlet boundary condition on the interface  $\Gamma$ :

$$p_p = \lambda, \quad \text{on } \Gamma \times (0, T).$$
 (4.5)

Its variational formulation is given by:

For a.e.  $t \in (0, T)$ , find  $(\mathbf{u}_p(t), p_p(t)) \in \mathbf{X}_p \times Q_p$  such that:

$$a_p(\boldsymbol{u}_p, \boldsymbol{v}_p) - b_p(\boldsymbol{v}_p, p_p) = -b_{\Gamma p}(\boldsymbol{v}_p, \lambda), \qquad \forall \boldsymbol{v}_p \in \boldsymbol{X}_p,$$
 (4.6)

$$b_p(\mathbf{u}_p, q_p) + (S_p \partial_t p_p, q_p) = (f_p, q_p)_{\Omega_p}, \qquad \forall q_p \in Q_p, \tag{4.7}$$

with the initial condition

$$p_p(\cdot,0) = p_{p0}, \quad \text{in } \Omega_p. \tag{4.8}$$



For given  $f_p \in L^2(0, T; Q_p)$ ),  $\lambda \in L^2(0, T; \Lambda)$  and  $p_{p0} \in H^1(\Omega_p)$ , there exists a unique solution

$$(\boldsymbol{u}_p, p_p) \in L^2(0, T; \boldsymbol{X}_p) \times H^1(0, T; Q_p)$$

to (4.6)–(4.7) with the initial condition (4.8). This is obtained by using the strong monotonicity of the viscosity function (2.4) and the Faedo–Galerkin method for mixed formulations of the Darcy problem as in [43].

#### 4.3 Nonlinear Space-Time Interface Problem

We first introduce the interface operators:

$$\begin{array}{l} \mathcal{S}_f \, : L^2(0,T;\Lambda) \longrightarrow L^2(0,T;\Lambda^*), \, S_f(\lambda) = \boldsymbol{u}_f(\lambda) \cdot \boldsymbol{n}_f|_{\Gamma}, \\ \mathcal{S}_p \, : L^2(0,T;\Lambda) \longrightarrow L^2(0,T;\Lambda^*), \, S_p(\lambda) = \boldsymbol{u}_p(\lambda) \cdot \boldsymbol{n}_p|_{\Gamma}, \end{array}$$

where  $(\boldsymbol{u}_f(\lambda), p_f(\lambda))$  and  $(\boldsymbol{u}_p(\lambda), p_p(\lambda))$  are the solutions to the Stokes problem (4.2)–(4.4) and the Darcy problem (4.6)–(4.8) respectively.

As the continuity of the normal stress (2.5b) is imposed via  $\lambda$  in (4.1) and (4.5) (note that the Beaver–Joseph–Saffmann condition is imposed naturally in (4.2)), there remains to enforce the condition (2.5a), which leads to the interface problem: Find  $\lambda \in L^2(0, T; \Lambda)$  such that:

$$\int_{0}^{T} \left( \left\langle S_{f}(\lambda), \zeta \right\rangle_{\Gamma} + \left\langle S_{p}(\lambda), \zeta \right\rangle_{\Gamma} \right) ds = 0, \quad \forall \zeta \in L^{2}(0, T; \Lambda). \tag{4.9}$$

This is a time-dependent and nonlinear problem which will be solved by a nested iteration approach. Toward that end, we define the operator:

$$\Psi(\lambda) := S_f(\lambda) + S_p(\lambda), \tag{4.10}$$

and apply the Newton algorithm to (4.9) to obtain the following linear system at each iteration k:

$$\int_0^T \left\langle \Psi'(\lambda^k)(\lambda^{k+1} - \lambda^k), \zeta \right\rangle_{\Gamma} ds = \int_0^T \left\langle -\Psi(\lambda^k), \zeta \right\rangle_{\Gamma} ds, \quad \forall \zeta \in L^2(0, T; \Lambda), \quad (4.11)$$

where  $\Psi'(\lambda)(h) = S_{f,\lambda}^{\text{lin}}(h) + S_{p,\lambda}^{\text{lin}}(h)$ , and

$$S_{f,\lambda}^{\text{lin}}(h) = \boldsymbol{w}_f(h) \cdot \boldsymbol{n}_f|_{\Gamma}, \quad S_{p,\lambda}^{\text{lin}}(h) = \boldsymbol{w}_p(h) \cdot \boldsymbol{n}_p)|_{\Gamma},$$

in which  $(\boldsymbol{w}_f(h), \xi_f(h))$  is the solution to the linearized Stokes problem [51]:

$$(\partial_{t}\boldsymbol{w}_{f},\boldsymbol{v}_{f}) + (v_{f}(|\boldsymbol{D}(\boldsymbol{u}_{f})|)\boldsymbol{D}(\boldsymbol{w}_{f}),\boldsymbol{D}(\boldsymbol{v}_{f}))$$

$$+ \left(\frac{(r_{f}-2)(v_{f0}-v_{f\infty})K_{f}}{(1+K_{f}|\boldsymbol{D}(\boldsymbol{u}_{f})|^{2-r_{f}})^{2}|\boldsymbol{D}(\boldsymbol{u}_{f})|^{r_{f}}}\boldsymbol{D}(\boldsymbol{u}_{f})(\boldsymbol{D}(\boldsymbol{u}_{f}):\boldsymbol{D}(\boldsymbol{w}_{f})),\boldsymbol{D}(\boldsymbol{v}_{f})\right)$$

$$-(\xi_{f},\nabla\cdot\boldsymbol{v}_{f}) + \sum_{j=1}^{d-1}c_{BJS}(\boldsymbol{w}_{f}\cdot\boldsymbol{t}_{j},\boldsymbol{v}_{f}\cdot\boldsymbol{t}_{j})_{\Gamma} = -\langle h,\boldsymbol{v}_{f}\cdot\boldsymbol{n}_{f}\rangle_{\Gamma}, \quad \forall \boldsymbol{v}_{f}\in\boldsymbol{X}_{f}, \quad (4.12)$$

$$(q_{f},\nabla\cdot\boldsymbol{w}_{f}) = 0, \quad \forall q_{f}\in Q_{f}, \quad (4.13)$$

and  $(\boldsymbol{w}_n(h), \xi_n(h))$  is the solution to the linearized Darcy problem:

$$(S_p \partial_t \xi_p, q_p) + (q_p, \nabla \cdot \boldsymbol{w}_p) = 0, \quad \forall q_p \in Q_p, \tag{4.14}$$



$$\left(\nu_{\text{eff}}(|\boldsymbol{u}_{p}|) \kappa^{-1} \boldsymbol{w}_{p}, \boldsymbol{v}_{p}\right) + \left(\frac{(r_{p} - 2)(\nu_{p0} - \nu_{p\infty}) K_{p}}{(1 + K_{p}|\boldsymbol{u}_{p}|^{2 - r_{p}})^{2} |\boldsymbol{u}_{p}|^{r_{p}}} \boldsymbol{u}_{p}(\boldsymbol{u}_{p} : \boldsymbol{w}_{p}), \boldsymbol{v}_{p}\right) - (\xi_{p}, \nabla \cdot \boldsymbol{v}_{p})$$

$$= -\langle h, \boldsymbol{v}_{p} \cdot \boldsymbol{n}_{p} \rangle_{\Gamma}, \quad \forall \boldsymbol{v}_{p} \in \boldsymbol{X}_{p}, \tag{4.15}$$

Note that  $\mathbf{u}_f = \mathbf{u}_f(\lambda)$  in (4.12) and  $\mathbf{u}_p = \mathbf{u}_p(\lambda)$  in (4.15). The nested iteration algorithm for solving (4.9) is summarized in Algorithm 1.

#### Algorithm 1 - Nested Iteration Approach

**Input**:  $\lambda^0$  initial guess,  $\epsilon$  tolerance and  $N_{\text{iter}}$  maximum number of iterations. **Output**:  $\lambda^k$ 

k = 0, error = 0,

while  $k < N_{\text{iter}}$  and error  $> \epsilon$ , do:

1: Compute the RHS of (4.11) by solving the nonlinear Stokes problem (4.2)-(4.3) and the nonlinear Darcy problem (4.6)-(4.7) with  $\lambda = \lambda^k$ :

$$\Psi(\lambda^k) = \mathcal{S}_f(\lambda^k) + \mathcal{S}_p(\lambda^k).$$

2: Solve the linearized interface problem with a Krylov-type method (e.g., GMRES):

$$\int_0^T \left\langle \Psi'(\lambda^k)(h^k), \zeta \right\rangle_\Gamma \, ds = \int_0^T \left\langle -\Psi(\lambda^k), \zeta \right\rangle_\Gamma \, ds, \quad \forall L^2(0, T; \Lambda),$$

where the left-hand side is given by

$$\Psi'(\lambda^k)(h^k) = S_{f,\lambda^k}^{\text{lin}}(h^k) + S_{p,\lambda^k}^{\text{lin}}(h^k).$$

That means each Krylov-iteration involves solution of linearized problems (4.12)-(4.15) to compute the matrix-free vector product on the left-hand side.

3: Update  $\lambda^{k+1} = \lambda^k + h^k$ , k = k + 1, error  $= \|h^k\|$ .

The linearized interface problem (4.11) can be preconditioned by using the inverse operator of  $S_{f,\lambda}^{\mathrm{lin}}$  as proposed for the stationary case in [24]. That corresponds to solving the linearized Stokes problem with given normal velocity on the interface as Dirichlet boundary condition, and computing the normal stress on the interface.

Remark 1 Unlike the steady case [22], the time-dependent Steklov-Poincaré operators for the Stokes-Darcy system are nonsymmetric. Thus a direct proof of the existence and uniqueness of the solution of the space-time interface problem (4.9) does not follow in a standard way, and remains an open problem. In fact, this is also the case for homogeneous domain decomposition (i.e. the same equation type is imposed in the subdomains) as pointed out in [43]; generally there is no analysis on the convergence of the iterative method for solving the space-time interface problem with the Steklov-Poincaré operator. In [48], convergence of a Richardson iteration method for the heat equation was proved using detailed properties of the Green's function; however, generalization of such analysis to the case of heterogeneous media (i.e. with discontinuous coefficients) is difficult.

## 5 Nonconforming Discretization in Time

As we solve the nonlinear interface problem (4.9) globally in time, different time discretization schemes and/or different time step sizes can be used in the Stokes and Darcy regions. At



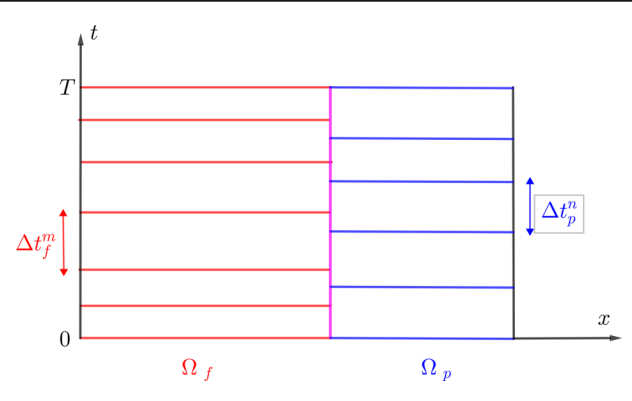


Fig. 2 Nonconforming time grids for the Stokes and Darcy problems

the space-time interface, data is transferred from one space-time subdomain to a neighboring subdomain by using a suitable projection.

We consider semi-discrete problems in time with nonconforming time grids. Let  $\mathcal{T}_f$  and  $\mathcal{T}_p$  be two possibly different partitions of the time interval (0, T) into sub-intervals (see Fig. 2):

$$\mathcal{T}_f = \bigcup_{m=1}^M J_f^m$$
, with  $J_f^m = (t_f^{m-1}, t_f^m]$ , and  $\mathcal{T}_p = \bigcup_{n=1}^N J_p^n$ , with  $J_p^n = (t_f^{n-1}, t_f^n]$ .

The time step sizes are  $\Delta t_f^m = t^m - t^{m-1}$ , m = 1, ..., M, and  $\Delta t_p^n = t^n - t^{n-1}$ , n = 1, ..., N, in the Stokes and Darcy regions, respectively. To simplify the discussion, the same temporal discretization scheme is considered for both subproblems; we use the backward Euler method for the time discretization and obtain the following semi-discrete local problems for the free flow

$$\left(\frac{\boldsymbol{u}_{f}^{m} - \boldsymbol{u}_{f}^{m-1}}{\Delta t_{f}^{m}}, \boldsymbol{v}_{f}\right)_{\Omega_{f}} + a_{f}(\boldsymbol{u}_{f}^{m}, \boldsymbol{v}_{f}) - b_{f}(\boldsymbol{v}_{f}, p_{f}^{m})$$

$$= (\boldsymbol{f}_{f}^{m}, \boldsymbol{v}_{f})_{\Omega_{f}} - b_{\Gamma f}(\boldsymbol{v}_{f}, \lambda^{m}), \qquad \forall \boldsymbol{v}_{f} \in \boldsymbol{X}_{f}, \qquad (5.1)$$

$$b_{f}(\boldsymbol{u}_{f}^{m}, q_{f}) = 0, \qquad \forall q_{f} \in Q_{f}, \qquad (5.2)$$

and the Darcy flow

$$a_p(\boldsymbol{u}_p^n, \boldsymbol{v}_p) - b_p(\boldsymbol{v}_p, p_p^n) = -b_{\Gamma p}(\boldsymbol{v}_p, \lambda^n), \quad \forall \boldsymbol{v}_p \in \boldsymbol{X}_p,$$
 (5.3)

$$b_p(\boldsymbol{u}_p^n, q_p) + \left(S_p \frac{p_p^n - p_p^{n-1}}{\Delta t_p^n}, q_p\right) = (f_p^n, q_p)_{\Omega_p}, \quad \forall q_p \in Q_p.$$
 (5.4)

The wellposedness of the decoupled semi-discrete Stokes and Darcy problems (5.1)–(5.4) is followed from the strong monotonicity of the viscosity functions (2.2) and (2.4), and [29]. The same idea can be generalized to higher order methods [41].

For i = f or i = p, we denote by  $P_0(\mathcal{T}_i, \Lambda)$  the space of piecewise constant functions in time on grid  $\mathcal{T}_i$  with values in  $\Lambda$ :

$$P_0(\mathcal{T}_f, \Lambda) = \left\{ \phi : (0, T) \to \Lambda, \phi \text{ is constant on } J_f^m, \ \forall m = 1, \dots, M \right\},$$

$$P_0(\mathcal{T}_p, \Lambda) = \left\{ \phi : (0, T) \to \Lambda, \phi \text{ is constant on } J_p^n, \ \forall n = 1, \dots, N \right\}.$$
(5.5)

In order to exchange data on the space-time interface between different time grids, we define the following  $L^2$  projection  $\Pi_{p,f}$  from  $P_0(\mathcal{T}_f,\Lambda)$  onto  $P_0(\mathcal{T}_p,\Lambda)$  (see [33,41]): for  $\phi \in$  $P_0(\mathcal{T}_f, \Lambda), \Pi_{p,f} \phi |_{J_p^n}$  is the average value of  $\phi$  on  $J_p^n$ , for  $n = 1, \ldots, N$ :

$$\Pi_{p,f}(\phi)|_{J_p^n} = \frac{1}{|J_p^n|} \sum_{m=1}^M \int_{J_p^n \cap J_f^m} \phi.$$
 (5.6)

The projection  $\Pi_{f,p}$  from  $P_0(\mathcal{T}_p,\Lambda)$  onto  $P_0(\mathcal{T}_f,\Lambda)$  can be defined similarly. We use the algorithm described in [33] for effectively performing these projections.

Next, we weakly enforce the transmission conditions over the time intervals with nonconforming time grids. We still denote by  $(\boldsymbol{u}_f, p_f)$  and  $(\boldsymbol{u}_p, p_p)$  the solution of the semi-discrete in time problems. We choose  $\lambda$  piecewise constant in time on one grid, either  $\mathcal{T}_f$  or  $\mathcal{T}_p$ . For the Stokes-Darcy coupling, the flow is supposed to be faster in the fluid domain than that in the porous medium, thus we choose  $\lambda \in P_0(\mathcal{T}_f, \Lambda)$  and impose

$$\left(-\boldsymbol{n}_f \cdot (\boldsymbol{v}_f(|\boldsymbol{D}(\boldsymbol{u}_f)|)\boldsymbol{D}(\boldsymbol{u}_f)) \cdot \boldsymbol{n}_f + p_f\right)|_{\Gamma} = \Pi_{f,f}(\lambda) = \lambda.$$

The weak continuity of the normal stress in time across the interface is fulfilled by letting

$$p_p|_{\Gamma} = \Pi_{p,f}(\lambda) \in P_0(\mathcal{T}_p, \Lambda).$$

The semi-discrete (nonconforming in time) counterpart of the normal velocity continuity (2.5a) is weakly enforced by integrating it over each time interval  $J_f^m$  of grid  $\mathcal{T}_f$ :  $\forall m = 1, ..., M,$ 

$$\int_{J_{x}^{m}} \left( \left\langle S_{f}(\lambda), \zeta \right\rangle_{\Gamma} + \left\langle \Pi_{f, p} \left( S_{p} \left( \Pi_{p, f}(\lambda) \right) \right), \zeta \right\rangle_{\Gamma} \right) ds = 0, \quad \forall \zeta \in \Lambda.$$
 (5.7)

Similarly for the linearized interface problem:

$$\int_{J_{f}^{m}} \left( \left\langle S_{f,\lambda^{k}}^{\text{lin}}(h^{k}), \zeta \right\rangle_{\Gamma} + \left\langle \Pi_{f,p} \left( S_{p,\lambda^{k}}^{\text{lin}}(\Pi_{p,f}(h^{k})), \zeta \right)_{\Gamma} \right) ds$$

$$= \int_{J_{f}^{m}} \left( \left\langle -S_{f}(\lambda^{k}), \zeta \right\rangle_{\Gamma} + \left\langle -\Pi_{f,p} \left( S_{p} \left( \Pi_{p,f}(\lambda^{k}) \right) \right), \zeta \right\rangle_{\Gamma} \right) ds, \quad \forall \zeta \in \Lambda. \tag{5.8}$$

In the next section, we shall investigate the numerical performance of the nonconforming time grids in terms of accuracy, efficiency and long-term stability.

#### **6 Numerical Results**

We investigate the numerical performance of the proposed global-in-time decoupling algorithm on two test cases: Test case 1 with a known solution and Test case 2 where the flow is driven by a pressure drop. For the latter, we consider both continuous and discontinuous parameters. We shall verify the accuracy in space and in time, the efficiency of the proposed method with nonconforming time grids over conforming time grids, and the long-time stability of the proposed method. Note that the code to generate the results below is implemented in FreeFem++ [42] in a sequential setting, and we do not investigate parallel performance of the method in this work.



#### 6.1 Test Case 1: With a Known Analytical Solution

We consider a test case with a known exact solution. The fluid domain and porous medium are  $\Omega_f = (0, 1) \times (1, 2)$  and  $\Omega_p = (0, 1) \times (0, 1)$  respectively, and the exact solution is given by

$$\begin{split} & \mathbf{u}_f = \left[ (y-1)^2 x^3 (1+t^2), \; -\cos(y) e (1+t^2) \right], \\ & p_f = \left( \cos(x) e^y + y^2 - 2y + 1 \right) \left( 1 + t^2 \right), \\ & \mathbf{u}_p = \left[ -x \left( \sin(y) e + 2 (y-1) \right) \left( 1 + t^2 \right), \; \left( -\cos(y) e + (y-1)^2 \right) \left( 1 + t^2 \right) \right], \\ & p_p = \left( -\sin(y) e + \cos(x) e^y + y^2 - 2y + 1 \right) \left( 1 + t^2 \right), \end{split}$$

for which the Beavers–Joseph–Saffman condition is satisfied with  $\alpha=1$ . We perform the numerical experiments with the following parameters:  $\kappa=1$ ,  $S_p=1$ ,  $K_f=K_p=1$ ,  $v_{f\infty}=v_{p\infty}=0.5$  and  $v_{f0}=v_{p0}=1.5$ . The boundary and initial conditions are imposed using the exact solution. For finite element approximations, we consider structured meshes and use either (i) the Taylor–Hood elements for both Stokes and Darcy problems or (ii) the MINI elements for the Stokes problem and the Raviart-Thomas elements of order one and P1 elements (RT1-P1) for the Darcy problem. In addition, a stability term  $\eta\left(\nabla \cdot \boldsymbol{u}_p, \nabla \cdot \boldsymbol{v}_p\right)$  was added to the Darcy equation with  $\eta=10$  as the exact Darcy velocity field is divergence free.

We shall verify the convergence rates in space and in time of the proposed algorithm with nonconforming time grids. For the iterative solvers, unless otherwise specified, only one Newton iteration is performed (i.e., k = 1 in Algorithm 1) and GMRES stops when the relative residual is smaller than the tolerance  $\varepsilon = 10^{-7}$  or when the maximum number of iterations, itermax = 100, is reached. We first investigate the accuracy in space for both linear viscosities with  $r_f = r_p = 2$  and nonlinear viscosities with  $r_f = r_p = 1.5$ . Tables 1 and 2 show the errors at T=0.01 with  $\Delta t_f=0.002$  and  $\Delta t_p=0.001$  for the linear and nonlinear problems using different finite element spaces. As this is a non-physical example, we have chosen a large time step in the fluid domain and a small time step in the porous medium. In the next test case, we will consider the choice where the time step size in the fluid domain is smaller. We observe from Tables 1 and 2 that the orders of accuracy in space are preserved with nonconforming time grids. In addition, concerning the convergence of GMRES to solve the linearized interface problem, we show in Table 3 the number of GMRES iterations needed to reach the tolerance  $\varepsilon = 10^{-10}$  for the case with no preconditioner and with the preconditioner  $\left(S_{f,\lambda}^{\text{lin}}\right)^{-1}$ . First, we notice the number of iterations required is reasonable; for the case without preconditioner, it is increasing slightly when the mesh size is decreasing while for the preconditioned system, the number of iterations remain small when h is small.

For time errors, we analyze the accuracy in time when nonconforming time grids are used. Toward this end, we fix h = 1/32 and denote by  $\Delta t_{\rm coarse} \in \{0.2, 0.1, 0.05, 0.025\}$  the coarse time step sizes, and  $\Delta t_{\rm fine} = \Delta t_{\rm coarse}/2$  the fine time step size. We consider three types of time grids as follows:

- i) Coarse conforming time grids:  $\Delta t_f = \Delta t_p = \Delta t_{\text{coarse}}$
- ii) Fine conforming time grids:  $\Delta t_f = \Delta t_p = \Delta t_{\text{fine}}$ .
- iii) Nonconforming time grids:  $\Delta t_f = \Delta t_{\text{coarse}}$  and  $\Delta t_p = \Delta t_{\text{fine}}$ .

We first consider the approximations by Taylor-Hood elements. Figures 3 and 4 show the errors for the linear and nonlinear viscosities respectively. We observe that first order convergence is preserved with the nonconforming time grids. Moreover, the errors with



 
 Table 1 [Test case 1] Errors with Taylor–Hood elements for the Stokes and Darcy problems at T=0.01 with
  $\Delta t_f = 0.002$  and  $\Delta t_p = 0.001$ 

h		1/4	1/8		1/16		1/32	
Linea	ır viscosities							
$\boldsymbol{u}_f$	$L^2$ error	9.07e-04	9.33e-05	[3.28]	1.19e-05	[2.97]	1.79e-06	[2.73]
	$H^1$ error	2.64e-02	5.55e-03	[2.25]	1.38e-03	[2.01]	3.72e-04	[1.89]
$p_f$	$L^2$ error	2.91e-02	5.55e-03	[2.39]	1.36e-03	[2.03]	3.97e-04	[1.78]
$\boldsymbol{u}_p$	$L^2$ error	1.29e-03	1.71e-04	[2.92]	2.02e-05	[3.08]	4.58e-06	[2.14]
	$H^{ m div}$ error	2.24e-03	3.42e-04	[2.71]	8.19e-05	[2.06]	1.93e-05	[2.09]
$p_p$	$L^2$ error	3.12e-02	5.07e-03	[2.62]	1.34e-03	[1.92]	3.24e-04	[2.05]
Nonli	inear viscosities							
$\boldsymbol{u}_f$	$L^2$ error	9.64e-04	1.03e-04	[3.23]	1.82e-05	[2.50]	1.26e-05	
	$H^1$ error	2.77e-02	5.88e-03	[2.24]	1.47e-03	[2.00]	4.18e-04	[1.81]]
$p_f$	$L^2$ error	2.84e-02	5.50e-03	[2.37]	1.50e-03	[1.88]	7.36e-04	[1.03]
$\boldsymbol{u}_p$	$L^2$ error	1.26e-03	1.72e-04	[2.87]	2.10e-05	[3.03]	7.44e-06	
	$H^{ m div}$ error	2.18e-03	3.37e-04	[2.69]	8.00e-05	[2.08]	1.98e-05	[2.02]
$p_p$	$L^2$ error	3.02e-02	4.91e-03	[2.62]	1.30e-03	[1.92]	3.15e-04	[2.05]

Table 2 [Test case 1] Errors with MINI elements for the Stokes problem and with RT1-P1 elements for the Darcy problem at T=0.01 with  $\Delta t_f=0.002$  and  $\Delta t_p=0.001$ 

h		1/4	1/8		1/16		1/32	
Linea	r viscosities							
$\boldsymbol{u}_f$	$L^2$ error	1.09e-02	2.63e-03	[2.05]	6.72e-04	[1.97]	1.82e-04	[1.89]
	$H^1$ error	2.24e-01	9.88e-02	[1.18]	5.02e-02	[0.98]	2.69e-02	[0.90]
$p_f$	$L^2$ error	2.51e-01	6.65e-02	[1.92]	2.22e-02	[1.58]	1.06e-02	[1.07]
$\boldsymbol{u}_p$	$L^2$ error	2.11e-02	4.29e-03	[2.30]	1.10e-03	[1.96]	2.65e-04	[2.05]
	$H^{ m div}$ error	2.36e-02	5.03e-03	[2.23]	1.28e-03	[1.97]	3.12e-04	[2.04]
$p_p$	$L^2$ error	3.04e-02	4.94e-03	[2.62]	1.31e-03	[1.92]	3.16e-04	[2.05]
Nonli	near viscosities							
$\boldsymbol{u}_f$	$L^2$ error	1.09e-02	2.62e-03	[2.05]	6.70e-04	[1.97]	1.81e-04	[1.89]
	$H^1$ error	2.24e-01	9.88e-02	[1.18]	5.02e-02	[0.98]	2.69e-02	[0.90]
$p_f$	$L^2$ error	2.07e-01	5.40e-02	[1.94]	1.86e-02	[1.54]	8.79e-03	[1.08]
$\boldsymbol{u}_p$	$L^2$ error	2.12e-02	4.30e-03	[2.30]	1.10e-03	[1.97]	2.66e-04	[2.05]
	$H^{ m div}$ error	2.37e-02	5.02e-03	[2.24]	1.28e-03	[1.97]	3.12e-04	[2.04
$p_p$	$L^2$ error	2.95e-02	4.79e-03	[2.63]	1.27e-03	[1.92]	3.08e-04	[2.04]

nonconforming time grids (in magenta) in the porous medium are close to those with fine conforming time steps (in red), which is expected as a smaller time step is used in the porous medium. Likewise, the errors with nonconforming time grids (in magenta) in the fluid domain are close to those with coarse conforming time steps (in blue). Thus the accuracy in time of the solution is preserved with the nonconforming time grids. Moreover, in Table 4, we compare



**Table 3** [Test case 1] Number of GMRES iterations needed to reach the tolerance  $10^{-10}$  using MINI elements for the Stokes problem and with RT1-P1 elements for the Darcy problem at T=0.01 with  $\Delta t_f=0.002$  and  $\Delta t_p=0.001$ 

h	Linear viscosities			Nonlinear viscosities				
	1/4	1/8	1/16	1/32	1/4	1/8	1/16	1/32
With no preconditioner	17	24	32	46	16	23	30	44
With a preconditioner	21	22	17	21	23	25	18	18

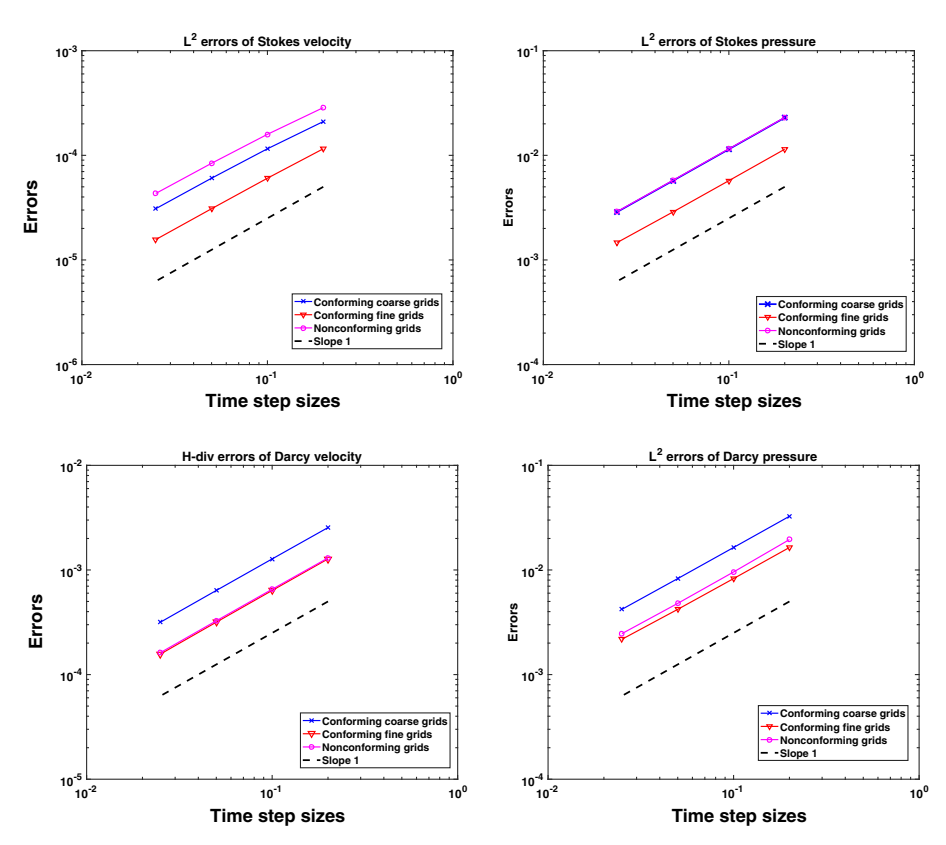


Fig. 3 [Test case 1] Errors for the linear Stokes and Darcy problems at T = 0.2 with Taylor–Hood elements

the computer running times when using conforming and nonconforming time grids, which shows that using nonconforming time grids could significantly reduce the computational time while still maintaining the desired accuracy.

We perform a similar test using MINI elements for the Stokes problem and RT1-P1 elements for the Darcy problem. We fix h=1/64, and consider  $\Delta t_{\rm coarse} \in \{0.8, 0.4, 0.2, 0.1\}$  and  $\Delta t_{\rm fine} = \Delta t_{\rm coarse}/2$ . The final time is large, T=0.8, thus we use two Newton iterations for the nonlinear solvers (instead of only one iteration). Figure 5 shows the errors for the case with nonlinear viscosities, which again confirms that the convergence order and accuracy in time are preserved with nonconforming time grids. In addition, we report in Table 5 the computer running times with conforming and nonconforming time grids on a fixed mesh



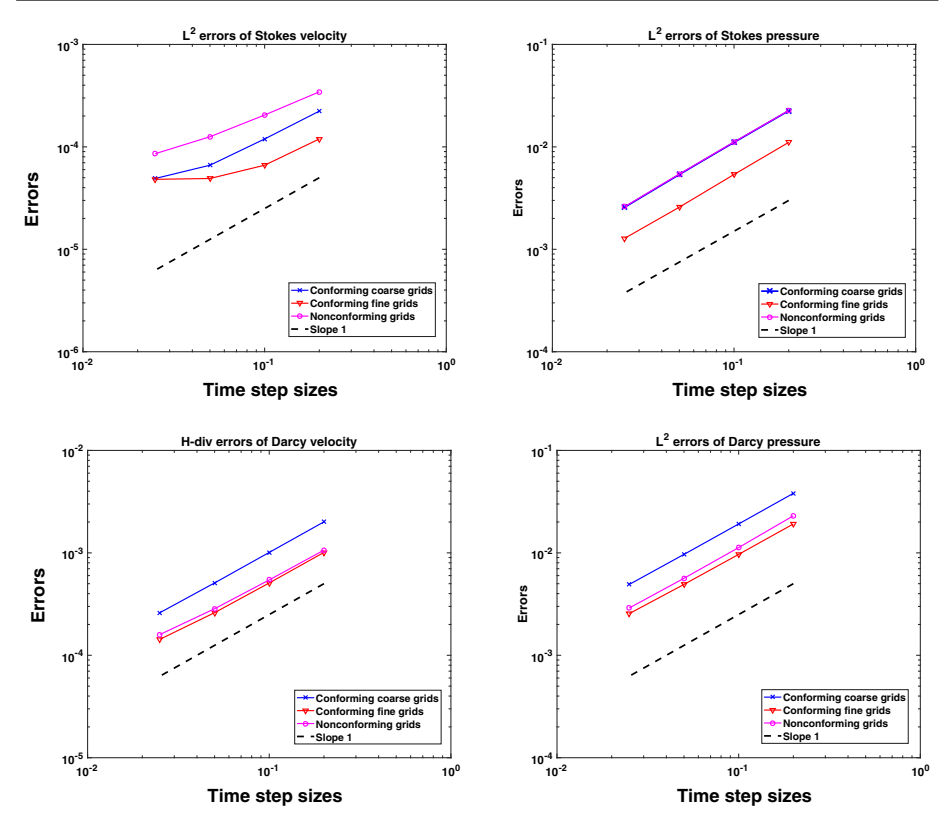


Fig. 4 [Test case 1] Errors for the nonlinear Stokes and Darcy problems at T=0.2 with Taylor–Hood elements

Table 4 Comparison of the computer running times (in seconds) of conforming and nonconforming time grids with Taylor–Hood elements on a fixed mesh h = 1/32

$\Delta t$	Linear viscosities		Nonlinear viscosi	ties
	Conforming	Nonconforming	Conforming	Nonconforming
0.2	87		122	
		143		178
0.1	209		287	
		285		348
0.05	432		578	
		578		710
0.025	893		1127	
		1176		1424
0.0125	1816		2175	

h = 1/32. We see that the use of nonconforming time grids is efficient in terms of accuarcy and computational cost.



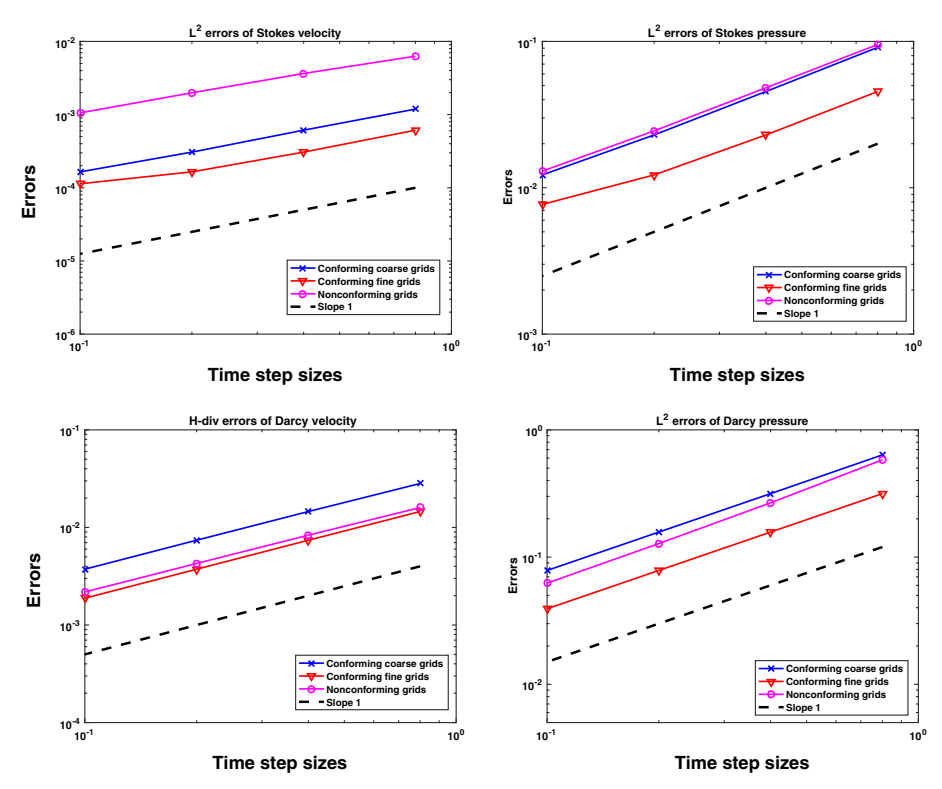


Fig. 5 [Test case 1] Errors for the nonlinear Stokes and Darcy problems at T=0.8 with MINI elements for the Stokes problem and RT1-P1 elements for the Darcy problem

**Table 5** Comparison of the computer running times (in seconds) of conforming and nonconforming time grids, with MINI elements for the Stokes problem and Raviart–Thomas elements for the Darcy problem on a fixed mesh h=1/32. Note that for the nonlinear viscosities, two Gauss–Newton iterations are performed

$\Delta t$	Linear viscosities		Nonlinear viscosit	ties
	Conforming	Nonconforming	Conforming	Nonconforming
0.8	72		167	_
		83		188
0.4	154		348	
		180		420
0.2	310		727	
		351		791
0.1	632		1447	
		697		1646
0.05	1262		2791	



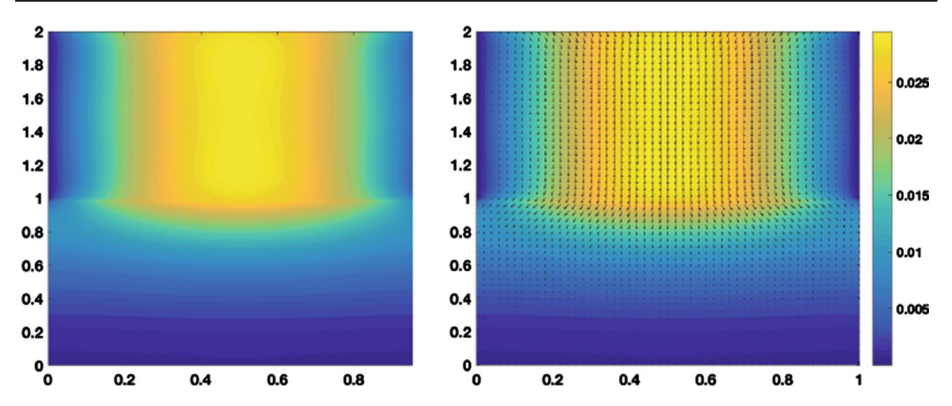


Fig. 6 [Test case 2] Velocity magnitude and velocity vector at T = 1

**Table 6** [Test case 2] Errors for the nonlinear Stokes and Darcy problems at T=1 with a fixed mesh size h = 1/32

Time step		$\boldsymbol{u}_f$		$p_f$		$\boldsymbol{u}_p$		$p_p$	
$\Delta t_f$	$\Delta t_p$	$H^1$ error		$L^2$ error		H <sup>div</sup> error		$L^2$ error	
1/4	1/2	3.44e-04		2.80e-03		4.56e-03		2.17e-03	
1/8	1/4	1.49e-04	[1.21]	1.37e-03	[1.03]	2.18e-03	[1.07]	1.12e-03	[0.95]
1/16	1/8	5.60e-05	[1.41]	6.51e-04	[1.07]	1.04e-03	[1.07]	5.48e-04	[1.03]
1/32	1/16	1.63e-05	[1.78]	2.95e-04	[1.14]	4.70e-04	[1.15]	2.53e-04	[1.12]

## 6.2 Test Case 2: Flow Driven by a Pressure Drop

In this test case, the flow is driven by a pressure drop: on the top boundary of  $\Omega_f$  we set  $p_{\rm in}=1$  and on the bottom boundary of  $\Omega_p$ ,  $p_{\rm out}=0$ , which is also chosen as the initial condition for the Darcy pressure. Along the left and right boundaries, we impose no-slip boundary condition for the Stokes flow and no-flow boundary condition for the Darcy flow. We also set zero velocity initial condition for the Stokes problem. The parameters are  $\kappa = 1$ ,  $K_f = K_p = 1, v_{f,\infty} = v_{p,\infty} = 1, v_{f,0} = v_{p,0} = 10, r_f = r_p = 1.35$  and  $\alpha = 1$ . The simulation time is T = 1. For this test case, we use cell conservative spatial discretization, i.e. MINI elements for the Stokes flow and RT1-P1 elements for the Darcy flow. The velocity magnitude and vector at the final time are shown Fig. 6.

We compute the reference solution on a mesh size h = 1/32 and  $\Delta t_{\text{ref}} = 0.01$ . We want to verify the convergence in time of the global-in-time domain decomposition method with nonconforming time grids:  $\Delta t_f = \Delta t_p/2$ . Table 6 shows the errors of the nonlinear Stokes and Darcy problems at T=1 with a fixed mesh size h=1/32, first order convergence in time is observed. In Tables 7 and 8, we compare the accuracy in time of the conforming and nonconforming time grids. In particular, the errors (with nonconforming time grids) in the fluid domain are close to those with fine conforming time steps, while those in the porous medium are close to those with coarse conforming time steps.

Next, we consider the case with discontinuous parameters. For the Stokes problem, we set  $K_f = 1$ ,  $\nu_{f,\infty} = 0.5$ ,  $\nu_{f,0} = 1$ , and for the Darcy problem,  $K_p = 0.001$ ,  $\nu_{p,\infty} = 0.001$ 1,  $v_{p,0} = 10$ . As before, we impose smaller time step in the fluid region and larger time step in the porous medium:  $\Delta t_f = \Delta t_p/2 = 0.125$ . The velocity magnitude at T = 1 is depicted



**Table 7** [Test case 2] Errors for the nonlinear Stokes problem at T = 1 with a fixed mesh size h = 1/32

Time grids	$\Delta t_f$	$\Delta t_p$	$\boldsymbol{u}_f$	$p_f$	
			$L^2$ error	$H^1$ error	$L^2$ error
Conforming coarse	1/8	1/8	3.01e-05	1.03e-04	6.71e-04
Nonconforming	1/16	1/8	1.64e-05	5.60e-05	6.51e-04
Conforming fine	1/16	1/16	1.38e-05	4.68e-05	3.08e-04

**Table 8** [Test case 2] Errors for the nonlinear Darcy problem at T = 1 with a fixed mesh size h = 1/32

Time grids	$\Delta t_f$	$\Delta t_p$	$\boldsymbol{u}_{P}$		$p_p$
			$L^2$ error	$H^{ m div}$ error	$L^2$ error
Conforming coarse	1/8	1/8	2.11e-04	1.05e-03	5.56e-04
Nonconforming	1/16	1/8	2.08e-04	1.04e-03	5.48e-04
Conforming fine	1/16	1/16	9.71-05	4.78e-04	2.59e-04

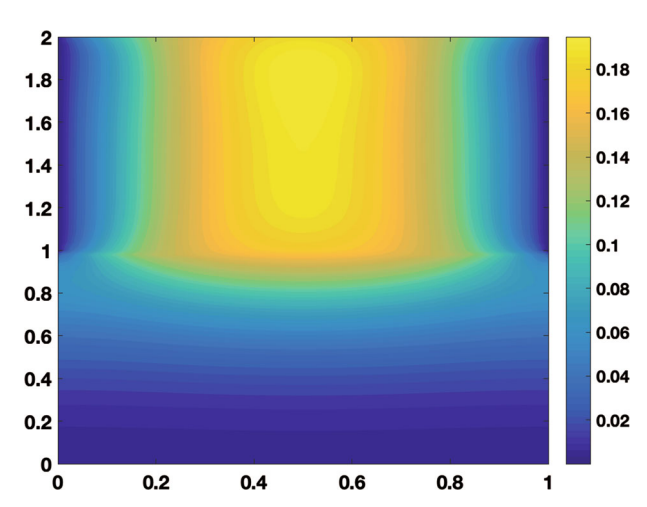


Fig. 7 [Test case 2 with discontinuous paramters] Velocity magnitude at T=1

in Fig. 7 and the errors are reported in Table 9, which again shows that the accuracy in time is well-preserved with nonconforming time grids.

Finally, we consider large jumps in the coefficients and long-time simulations. In particular, we lower the values of the storativity and permeability in the Darcy region while keeping all other parameters fixed:  $K_f=1$ ,  $v_{f,\infty}=0.5$ ,  $v_{f,0}=1$ ,  $K_p=10^{-6}$ ,  $v_{p,\infty}=1$ ,  $v_{p,0}=1.5$ . Three cases are considered: i)  $S_p=0.1$ ,  $\kappa=10^{-4}$ , ii)  $S_p=0.1$ ,  $\kappa=10^{-5}$ , and iii)  $S_p=0.01$ ,  $\kappa=10^{-5}$ . The mesh size is h=1/100 and the time step size in the Darcy region is four times larger than the one in the Stokes region:  $\Delta t_p=4\Delta t_f=0.5$ . The final time is T=100, thus we partition [0,T] into sub-intervals of smaller sizes, called time windows (see [41,43]); notice that successive time windows do not overlap in time. We perform the nested iteration on each time window sequentially in which the solution from the previous time window is used as the initial guess for the next time window. Figure 8 shows the magnitude



**Table 9** [Test case 2 with discontinuous parameters]  $L^2$ -errors for the nonlinear Stokes and Darcy problems at T = 1 with h = 1/32

Time grids	$\Delta t_f$	$\Delta t_p$	$u_f$	$p_f$	$u_p$	$p_p$
Conforming coarse	1/4	1/4	1.48e-03	2.02e-02	5.41e-03	1.45e-02
Nonconforming	1/8	1/4	2.33e-04	1.69e-02	4.70e-03	1.32e-02
Conforming fine	1/8	1/8	2.27e-04	1.00e-02	2.77e-03	7.63e-03

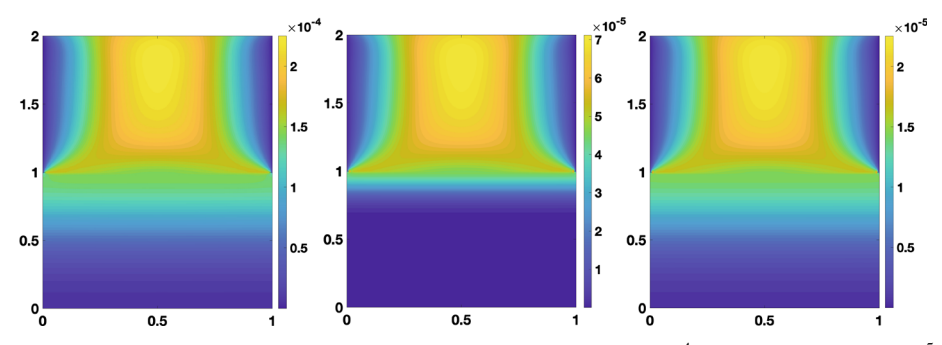


Fig. 8 [Test case 2] Velocity magnitude at T=100 with  $S_p=0.1, \kappa=10^{-4}$  (left),  $S_p=0.1, \kappa=10^{-5}$ (middle) and  $S_p = 0.01$ ,  $\kappa = 10^{-5}$  (right). Note that the color scale is different for each plot

of the velocity at T=100 for the different values of the parameters; note that the color scale is different for each plot. It is observed that the proposed space-time DD method is stable for long time simulations, and the velocity magnitude is much smaller for low permeability and storativity.

#### 7 Conclusion

We have introduced a decoupling scheme for the nonlinear Stokes–Darcy system, based on the time-dependent interface operators. The scheme is an implicit type that requires iterations between subdomains; the subproblems, time-dependent Stokes and Darcy equations, are solved using local time-stepping algorithms, respectively. The space-time domain decomposition method allows us to independently solve each subproblem using existing local solvers and enables the use of nonconforming time grids as well as different time-stepping algorithms for local problems. For numerical tests of the proposed algorithm two numerical examples were considered; the first is a non-physical problem with the known exact solution and the second is a flow problem driven by a pressure drop. Numerical results confirm that the algorithm simulates the model problem at the optimal order of accuracy and its efficiency is improved with the use of nonconforming time grids and the preconditioner for GMRES iterations. Although the model system is nonlinear, only one or two Newton iterations were needed within the given tolerance range, yielding the optimal accuracy in our test cases.

Some future directions for this work include extending the approach to more complex coupled problems such as the coupled Stokes-Darcy system with transport and a fluid flow coupled with a quasi-static poroelastic medium. In particular, because of the use of local time stepping, we expect that this approach is efficiently applicable to multiphysics problems, where local problems are in different time scales, e.g., fluid flows interacting with clays or



soils. Many such examples are found in applications of geomechanics and the quasi-static Biot's consolidation model [6] is often considered for a deformable porous medium. In the Biot model, the fluid motion in the porous medium is described by Darcy's law, while the deformation of the medium is governed by the linear elasticity. Interface conditions for the (Navier-)Stokes–Biot system are more complex than those of the Stokes–Darcy system, however, we expect that a similar approach can be considered for the large multiphysics problem to be turned into a time dependent Steklov–Poincaré operator equation. We are also currently investigating an optimized Schwartz waveform relaxation (OSWR) method using Robin transmission conditions for the Stokes–Darcy model considered in this work. Details concerning the development, analysis and numerical implementation of space-time domain decomposition based on OSWR is a subject of a forthcoming paper.

## References

- Arbogast, T., Brunson, D.S.: A computational method for approximating a Darcy-Stokes system governing a vuggy porous medium. Comput. Geosci. 11, 207–218 (2007)
- Arbogast, T., Gomez, M.S.M.: A discretization and multigrid solver for a Darcy-Stokes system of three dimensional vuggy porous media. Comput. Geosci. 13, 331–348 (2009)
- Badea, L., Discacciati, M., Quarteroni, A.: Numerical analysis of the Navier-Stokes/Darcy coupling. Numer. Math. 115, 195–227 (2010)
- 4. Beavers, G., Joseph, D.: Boundary conditions at a naturally impermeable wall. J. Fluid. Mech. 30, 197–207 (1967)
- Bernardi, C., Rebollo, T.C., Hecht, F., Mghazli, Z.: Mortar finite element discretization of a model coupling Darcy and Stokes equations, M2AN Math. Model. Numer. Anal. 42, 375–410 (2008)
- Biot, M.A.: Theory of elasticity and consolidation for a porous anisotropic solid. J. Appl. Phys. 25, 182–185 (1955)
- Burman, E., Hansbo, P.: A unified stabilized method for Stokes and Darcy's equations. J. Comput. Appl. Math. 198, 35–51 (2007)
- Cai, M., Mu, M.: A multilevel decoupled method for a mixed Stokes/Darcy model. J. Comput. Appl. Math. 236, 2452–2465 (2012)
- Cai, M., Mu, M., Xu, J.: Numerical solution to a mixed Navier-Stokes/Darcy model by the two-grid approach. SIAM J. Numer. Anal. 47, 3325–3338 (2009)
- Cai, M., Mu, M., Xu, J.: Preconditioning techniques for a mixed Stokes/Darcy model in porous media applications. J. Comput. Appl. Math. 233, 346–355 (2009)
- Caiazzo, A., John, V., Wilbrandt, U.: On classical iterative subdomain methods for the Stokes-Darcy problem. Comput. Geosci. 18, 711–728 (2014)
- Cao, Y., Gunzburger, M., He, X., Wang, X.: Robin-Robin domain decomposition methods for the steadystate Stokes-Darcy system with the Beavers-Joseph interface condition. Numer. Math. 117, 601–629 (2011)
- Cao, Y., Gunzburger, M., He, X., Wang, X.: Parallel, non-iterative, multi-physics domain decomposition methods for time-dependent Stokes-Darcy systems. Math. Comp. 83, 1617–1644 (2014)
- Cao, Y., Gunzburger, M., Hua, F., Wang, X.: Coupled Stokes-Darcy model with Beavers-Joseph interface boundary conditions. Commun. Math. Sci. 8, 1–25 (2010)
- Cao, Y., Gunzburger, M., Hu, X., Hua, F., Wang, X., Zhao, W.: Finite element approximations for Stokes-Darcy flow with Beavers-Joseph interface conditions. SIAM J. Numer. Anal. 47, 4239–4256 (2010)
- Cesmelioglu, A., Girault, V., Rivière, B.: Time-dependent coupling of Navier–Stokes and Darcy flows. ESAIM: M2AN 47, 539–554 (2013)
- Cesmelioglu, A., Rivière, B.: Primal discontinuous Galerkin methods for time dependent coupled surface and subsurface flow. J. Sci. Comput. 40, 115–140 (2009)
- Chen, W., Gunzburger, M., Hua, F., Wang, X.: A parallel Robin-Robin domain decomposition method for the Stokes–Darcy system. SIAM J. Numer. Anal. 49, 1064–1084 (2011)
- Chidyagwai, P., Ladenheim, S., Szyld, D.B.: Constraint preconditioning for the coupled Stokes–Darcy system. SIAM J. Sci. Comput. 38, 668–690 (2016)
- Chidyagwai, P., Rivière, B.: On the solution of the coupled Navier-Stokes and Darcy equations. Comput. Methods Appl. Mech. Engrg. 198, 3806–3820 (2009)



- 21. Chidyagwai, P., Rivière, B.: Numerical modelling of coupled surface and subsurface flow systems. Adv. Water Res. **33**, 92–105 (2010)
- 22. Discacciati, M.: Domain decomposition methods for the coupling of surface and groundwater flows, PhD dissertation, École Polytechnique Fédérale de Lausanne (2004)
- 23. Discacciati, M., Gerardo-Giorda, L.: Optimized Schwarz methods for the Stokes-Darcy coupling. IMA J. Numer. Anal. 38, 1959–1983 (2018)
- 24. Discacciati, M., Miglio, E., Quarteroni, A.: Mathematical and numerical models for coupling surface and groundwater flows. Appl. Numer. Math. 43, 57-74 (2002)
- 25. Discacciati, M., Quarteroni, A.: Analysis of a domain decomposition method for the coupling of Stokes and Darcy equations, In: F. Brezzi, A. Buffa, S. Corsaro, A. Murli (eds.) Numerical Mathematics and Advanced Applications, Springer Italia, Milan, pp. 3-20 (2003)
- 26. Discacciati, M., Quarteroni, A.: Convergence analysis of a subdomain iterative method for the finite element approximation of the coupling of Stokes and Darcy equations. Comput. Visual. Sci. 6, 93-103
- 27. Discacciati, M., Quarteroni, A.: Navier-Stokes/Darcy coupling: Modeling, analysis, and numerical approximation. Rev. Mat. Complut. 22, 315-426 (2009)
- Discacciati, M., Quarteroni, A., Valli, A.: Robin-Robin domain decomposition methods for the Stokes-Darcy coupling. SIAM J. Numer. Anal. 45, 1246–1268 (2007)
- 29. Ervin, V.J., Jenkins, E.W., Lee, H.: Approximation of the Stokes-Darcy system by optimization. J. Sci. Comput. 59, 775-794 (2014)
- 30. Ervin, V.J., Jenkins, E.W., Sun, S.: Coupled generalized nonlinear stokes flow with flow through a porous medium. SIAM J. Numer. Anal. 47, 929-952 (2009)
- 31. Ervin, V.J., Jenkins, E.W., Sun, S.: Coupling non-linear Stokes and Darcy flow using mortar finite elements. Appl. Numer. Math. 61, 1198–1222 (2011)
- 32. Gander, M.J., Halpern, L., Nataf, F.: Optimal Convergence for Overlapping and Non-Overlapping Schwarz Waveform Relaxation. In Proceedings of the 11th International Conference on Domain Decomposition Methods, Lai, C-H., Bjørstad, P., Cross, M., Widlund, O. (eds.), Domain Decomposition Press, Bergen, Norway, pp. 27-36 (1999)
- 33. Gander, M.J., Halpern, L., Nataf, F.: Optimal Schwarz waveform relaxation for the one dimensional wave equation. SIAM J. Numer. Anal. 41, 1643-1681 (2003)
- 34. Gander, M.J., Halpern, L.: Optimized Schwarz waveform relaxation methods for advection reaction diffusion problems. SIAM J. Numer. Anal. 45, 666-697 (2007)
- 35. Gander, M. J., Japhet, C., Maday, Y., Nataf, F.: A new cement to glue nonconforming grids with Robin interface conditions: The finite element case, in Domain Decomposition Methods in Science and Engineering, Lecture Notes in Computational Science and Engineering, vol. 40, Springer, Berlin, pp. 259-266 (2005)
- 36. Ganis, B., Vassilev, D., Wang, C., Yotov, I.: A multiscale flux basis for mortar mixed discretizations of Stokes-Darcy flows. Comput. Methods Appl. Mech. Engrg. 313, 259-278 (2017)
- 37. Galvis, J., Sarkis, M.: Non-matching mortar discretization analysis for the coupling Stokes–Darcy equations. Electron. Trans. Numer. Anal. 26, 350-384 (2007)
- Galvis, J., Sarkis, M.: FETI and BDD preconditioners for Stokes-Mortar-Darcy systems. Commun. Appl. Math. Comput. Sci. 5, 1–30 (2010)
- 39. Girault, V., Vassilev, D., Yotov, I.: A mortar multiscale finite element method for Stokes-Darcy flows. Numer. Math. 17, 93–165 (2014)
- Girault, V., Rivière, B.: DG approximation of coupled Navier-Stokes and Darcy equations by Beaver-Joseph-Saffman interface condition. SIAM J. Numer. Anal. 47, 2052–2089 (2009)
- 41. Halpern, L., Japhet, C., Szeftel, J.: Optimized Schwarz waveform relaxation and discontinuous Galerkin time stepping for heterogeneous problems. SIAM J. Numer. Anal. 50(5), 2588–2611 (2012)
- 42. Hecht, F.: New development in FreeFem++. J. Numer. Math. **20**, 251–265 (2012)
- 43. Hoang, T.T.P., Jaffré, J., Japhet, C., Kern, M., Roberts, J.E.: Space-time domain decomposition methods for diffusion problems in mixed formulations. SIAM J. Numer. Anal. 51(6), 3532-3559 (2013)
- Hoang, T.T.P., Japhet, C., Kern, M., Roberts, J.E.: Space-time domain decomposition for reduced fracture models in mixed formulation SIAM. J. Numer. Anal. 54, 288–316 (2016)
- 45. Hoang, T.T.P., Kunwar, H., Lee, H.: Nonconforming time discretization based on Robin transmission conditions for the Stokes-Darcy system, (2021), submitted
- Hoppe, R.H.W., Porta, P., Vassilevski, Y.: Computational issues related to iterative coupling of subsurface and channel flows. Calcolo 44, 1-20 (2007)
- 47. Jäger, W., Mikelíc, A.: On the boundary conditions at the contact interface between a porous medium and a free fluid. Ann. Sci. Norm. Super. Pisa Cl. Sci. 23, 403-465 (1996)



- Kwok, F.: Neumann–Neumann waveform relaxation for the time-dependent heat equation. Domain Decomposition Methods in Computational Science and Engineering XXI, Lecture Notes in Computational Science and Engineering 98, pp. 189–198, Springer-Verlag (2014)
- Layton, W., Schieweck, F., Yotov, I.: Coupling fluid flow with porous media flow. SIAM J. Numer. Anal. 40, 2195–2218 (2003)
- Layton, W., Tran, H., Trenchea, C.: Analysis of long time stability and errors of two partitioned methods for uncoupling evolutionary groundwater-surface water flows. SIAM J. Numer. Anal. 51, 248–272 (2013)
- Lee, H., Rife, K.: Least squares approach for the time-dependent nonlinear Stokes–Darcy flow. Comput. Math. Appl. 67, 1086–1815 (2014)
- Mardal, K.A., Tai, X.-C., Winther, R.: A robust finite element method for Darcy–Stokes flow. SIAM J. Numer. Anal. 40, 1605–1631 (2002)
- Márquez, A., Meddahi, S., Sayas, F.-J.: A decoupled preconditioning technique for a mixed Stokes–Darcy model. J. Sci. Comput. 57, 174–192 (2013)
- Mu, M., Xu, J.: A two-grid method of a mixed Stokes–Darcy model for coupling fluid flow with porous media flow. SIAM J. Numer. Anal. 45, 1801–1813 (2007)
- Mu, M., Zhu, X.H.: Decoupled schemes for a non-stationary mixed Stokes–Darcy model. Math. Comp. 79, 707–731 (2010)
- Quarteroni, A., Valli, A.: Domain Decomposition Methods for Partial Differential Equations. Clarendon Press, Oxford New York (1999)
- Rivière, B.: Analysis of a discontinuous finite element method for the coupled Stokes and Darcy problems.
   J. Sci. Comput. 22, 479–500 (2005)
- Rivière, B., Yotov, I.: Locally conservative coupling of Stokes and Darcy flows. SIAM J. Numer. Anal. 42, 1959–1977 (2005)
- Rui, H., Zhang, J.: A stabilized mixed finite element method for coupled Stokes and Darcy flows with transport. Comput. Methods. Appl. Mech. Engrg. 315, 169–189 (2017)
- Rybak, I., Magiera, J.: A multiple-time-step technique for coupled free flow and porous medium system.
   J. Comput. Phys. 272, 327–342 (2014)
- 61. Saffman, P.: On the boundary condition at the interface of a porous medium, *Stud. Appl. Math.* 1, pp. 93–101 (1971)
- 62. Shan, L., Zheng, H., Layton, W.: A decoupling method with different subdomain time steps for the nonstationary Stokes–Darcy model. Numer. Methods Partial Differ. Eqns. 29, 549–583 (2013)
- 63. Temam, R.: Navier-Stokes Equations: Theory and Numerical Analysis. Elsevier, North-Holland (1977)
- Toselli, A., Widlund, O.: Domain Decomposition Methods-Algorithms and Theory. Vol. 34 of Springer Series in Computational Mathematics. Springer-Verlag, Berlin (2005)
- Vassilev, D., Yotov, I.: Coupling Stokes–Darcy flow with transport. SIAM J. Sci. Comput. 31, 3661–3684 (2009)
- Vassilev, D., Wang, C., Yotov, I.: Domain decomposition for coupled Stokes and Darcy flows. Comput. Methods Appl. Mech. Engrg. 268, 264–283 (2014)

Publisher's Note Springer Nature remains neutral with regard to jurisdictional claims in published maps and institutional affiliations.

